Optimization of Electroactive Hydrogel Actuators

Megan L. O'Grady, Po-ling Kuo, and Kevin Kit Parker*

Disease Biophysics Group, Wyss Institute for Biologically-Inspired Engineering, School of Engineering and Applied Sciences, Harvard University

ABSTRACT To improve actuation of hydrogels, we utilized an emulsion polymerization to engineer porous structures into polyelectrolyte hydrogels. Porous hydrogels generated large deformation as a result of enhanced deswelling mechanisms; for instance, the decreased number of COO^- groups that must be protonated in porous hydrogels to initiate bending. Measurements of the mechanical properties revealed that porous hydrogels also bend to a larger extent because of their increased flexibility. Overall, our results demonstrate that the fast and large actuation of polyelectrolyte hydrogels can be accomplished by increasing the hydrogel porosity.

KEYWORDS: polyelectrolyte hydrogel • artificial muscle • actuation • hydrogel swelling • poly(acrylic acid)

Electroactuated polymer hydrogels are promising materials for soft robotic applications, because they are soft materials ($\sim$10 kPa elastic modulus) that require low voltages for actuation (1–5 V) and can be easily fabricated (1–4). The first hydrogel actuator used made a worm-like motion feasible by attaching both ends of the gel to a plastic ratchet bar (10). Since this seminal paper, hydrogels have been utilized extensively for artificial muscle applications (1–9). Hydrogel biomimetic actuators have been utilized to create mechanical hands (11), artificial fish (12) and various artificial muscle constructs (2, 4, 5, 13, 14). Moreover, an emerging trend is to incorporate lessons from biological materials into hydrogel actuators (1, 15). Because biological tissue is typically comprised of a porous media, we sought to further mimic this element of biological tissue and enhance the porosity of hydrogel artificial muscle constructs. Here we show that a reverse emulsion polymerization to create porous hydrogels can be utilized to significantly enhance the bending of electroactuated hydrogels.

In polyelectrolyte hydrogels, such as poly(sodium acrylate) (PAANa), hydrogel contraction depends on the repulsion of COO^- groups (13, 14, 16, 17), which is mediated by the exchange of H^+ ions. Because the electrostatic repulsion of COO^- groups is critically dependent on the concentration of COO^- moieties relative to COOH groups (13, 14, 16, 17), H^+ exchange determines the number of COOH groups in the polymer and thus initiates polymer swelling and deswelling. Therefore, the concentration of H^+ ions in solution (pH) is a critical determinant of polymer swelling and deswelling. We hypothesized that the actuation of PAANa gels could be

significantly improved by creating porous scaffolds to optimize the exchange of H^+ ions in PAANa hydrogels.

The goal of this study was to significantly enhance the bending of electroactuated hydrogels and explain the mechanisms underlying their large and rapid deformation. To increase PAANa hydrogel bending angles, an emulsion polymerization was utilized to create porous PAANa gels. Measurements of the stiffness and force generated by the gels revealed that porous hydrogels yield large bending angles due to their improved ability to stiffen in low pH (high H^+) conditions. In general, our results demonstrate that by creating porous hydrogel structures, the actuation of these hydrogels can be improved significantly.

METHODS

Preparation of Poly(sodium acrylate) Construct. We employed an emulsion templating technique to increase the hydrogel porosity (Figure 1a) (18). Initially, a 1% photoinitiator solution of Igracure 2959 (Ciba Specialty Chemicals, Tarrytown, NY) was prepared with 0.225 M maleic anhydride, 5.5 M NaOH, and 2.25 M Na_2PO_4 (Sigma-Aldrich, St. Louis, MO). Acrylic acid was added in a 7.3 M concentration and methylbisacrylamide was added in a 0.02 M concentration.

Emulsions were prepared using hexane, wherein 30 and 50% volume fractions of hexane/polymerization solution were produced and 0.15 M concentration of Tween 20 surfactant was added to the emulsion solution. In some cases, green 500 nm diameter polystyrene fluorescent beads (Invitrogen, Carlsbad California) were added in a 1% concentration to enhance imaging of the polymer bending trajectory. The polymerization solution was added to a plexiglass mold with 0.8 mm × 5 mm × 1 mm features and placed under UV light (XX-15MR Bench Lamp, 302 nm, UVP, Upland, CA). The gels were placed in acetone (Sigma-Aldrich, St. Louis, MO) to dissolve hexane and unpolymerized monomers present in the gels. Finally, the gels were equilibrated in a Normal Tyrode's (NT) solution at 19 °C, which is commonly used in cell electrophysiology studies. The NT was utilized to observe the behavior of the gel in physiological saline solutions. All components for the NT solution were purchased from Sigma Aldrich (St. Louis, MO). A NT solution was prepared with (in mmol/L) 135 NaCl, 5.4 KCl, 1.8 $CaCl_2$, 1
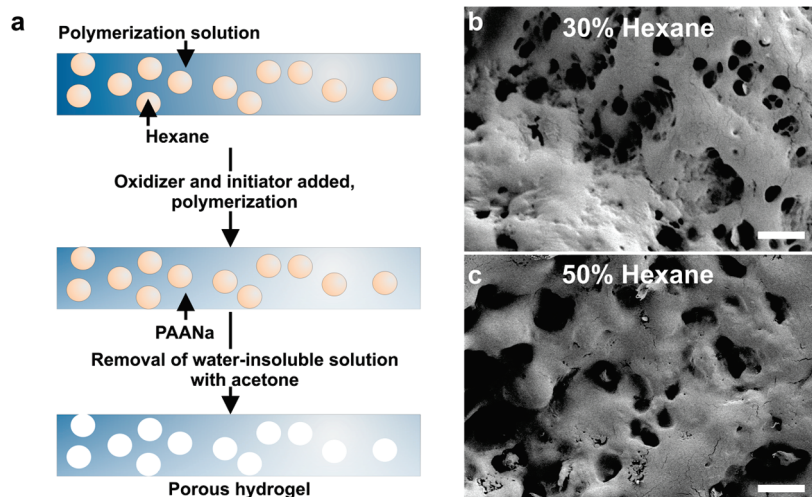
FIGURE 1. (a) Preparation of porous, electroactive hydrogels using emulsion polymerization. (b) Images of hexane droplets in a fluorescently labeled polymerization solution displayed a polydisperse distribution of pore sizes. (b, c) Scanning electron microscopy (SEM) images of porous PAANa hydrogels. The SEM image indicated large pores (>10 μm) using (b) 30 and (c) 50% hexane volume fractions with 0.15 M Tween 20 surfactant. Scale bar = 10 μm.
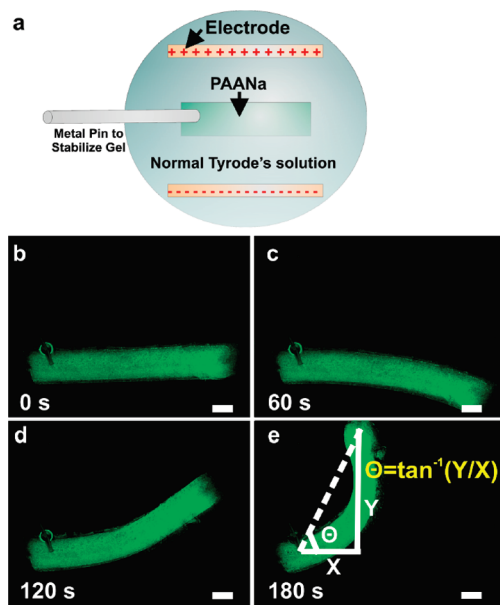

FIGURE 2. (a) Schematic of experimental setup where the gel sample is placed between two plate electrodes and 1.5–2.5 V/cm are applied. (b–e) The setup was utilized to image bending of fluorescently labeled PAANa constructs. Fluorescent labels were added to aid in the image analysis of bending trajectory. (e) The $X-Y$ position of the hydrogel end was used to calculate the bending angle. Scale bar = 1 mm.

MgCl$_2$, 0.33 NaH$_2$PO$_4$, 5 HEPES, and 5 glucose. The pH of the NT solution was 7.49 at 19 °C. The PAANa hydrogels were equilibrated in the NT solution at 19–23 °C for at least 20 h prior to an experiment.

Electroactuation Measurements. After equilibration in the NT solution, the PAANa gels were placed in a 35 mm Petri dish (Corning, Corning, NY) coated in a ~5 mm thick layer of polydimethylsiloxane (Dow Corning, Midland, MI). Platinized titanium electrodes (Idea Scientific Company, Minneapolis, MN) were placed 20 mm apart and connected to a DC power source (RSR Electronics, Avenel, NJ). As shown in Figure 2a, the PAANa gels were fixed at one end using a stainless steel minutien pin (Fine Science Tools, Foster City, CA). In some experiments, 0.02% phenol red (Sigma Aldrich, St. Louis, MO), a pH indicator, was added to the Normal Tyrode's.

Imaging was performed with a Zeiss M^2 Bio stereomicroscope (Carl Zeiss, Dresden, Germany) using a Zeiss AxioCam MRM camera at a frame rate of 1 frame/s (Figure 2b–e). As shown in Figure 2e, the X-Y position of the hydrogel end was calculated after application of 2.5 V/cm electric fields for 3 min. Image analyses were performed in MATLAB (MathWorks, Natick, MA). A two-sample t test ($p < 0.01$) was used to determined statistical significance.

Measurements of PAANa Deswelling. To quantify the extent of polymer deswelling, we placed PAANa gels in a 7.5 pH solution with 0.1 M Na$_2$PO$_4$ and 0.1 HEPES (Sigma-Aldrich, St. Louis, MO) pH buffers for 24 h. The gels were then placed in HEPES and Na$_2$PO$_4$ buffered pH solutions of 3.0. The mass of the gels after equilibration in a pH 7.5 solution was compared to the mass of the gels after 24 h in pH 3.0 solutions, and the % deswelling (D) was calculated as

$$D = \left| \frac{W_{\text{pH 3}} - W_{\text{pH 7.5}}}{W_{\text{pH 7.5}}} \right| \qquad (1)$$

where $W_{\text{pH 7.5}}$ represents the gel weight after equilibration in a pH 7.5 solution, and $W_{\text{pH 3}}$ represents the gel weight in pH 3.0.

Elasticity Measurements. An AR-G2 rheometer (TA Instruments, New Castle, DE) applied uniaxial compression to the PAANa gels to determine their mechanical properties. The maximum strain applied was 10%, which was prescribed at 50 μm/s. The PAANa gels were assumed to be linearly elastic based on the stress–strain curves (see the Supporting Information, Figure S1). The elastic modulus was determined by a least-squares fit of the linear portion (<10% strain) of the stress–strain curves.

RESULTS AND DISCUSSION

Preparation and Actuation of Porous, Electroactive Hydrogels. By creating porous hydrogels using emulsion templating (Figure 1b,c), bending angles of 70–80° were achieved with 2.5 V/cm electric field applied for 3 min (Figure 3). Our results indicated that for PAANa gels polymerized without an emulsion (Figure 3a–e), bending angles of 43.2 ± 14.8° (toward the anode) were achieved ($n = 13$, s.d.). However, PAANa gels polymerized in a 30% hexane
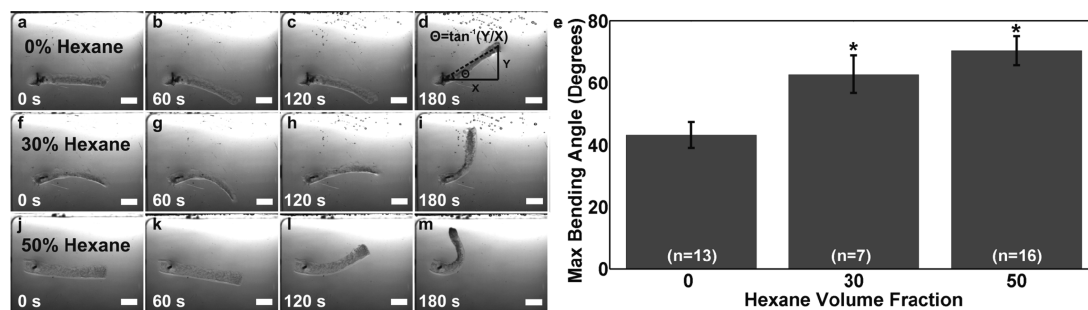
FIGURE 3. Hydrogels with varying hexane volume fractions in a Normal Tyrode's solution after (a, f, j) 0, (b,g,k) 60, (c, h, l) 120, and (d, i, m) 180 s. (e) Maximum bending angle vs hexane volume fraction after 180 s demonstrating that porous hydrogels bend to a larger degree. Error bars represent the standard error of the mean (s.e.m.) of the measurements, * indicates $p < 0.01$. Scale bar = 2 mm.
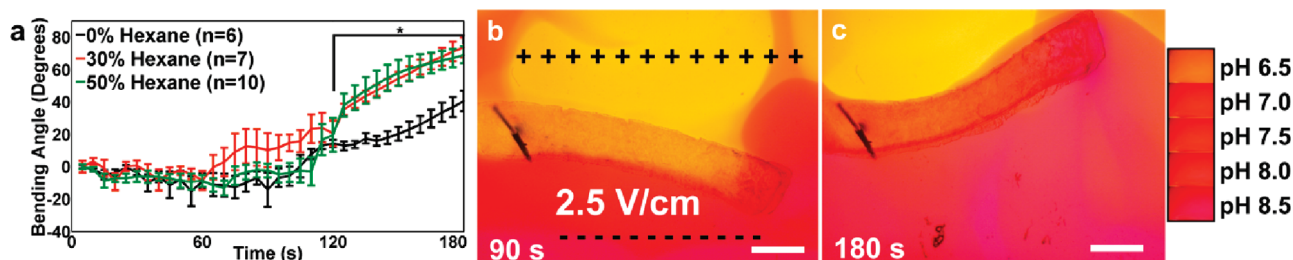

FIGURE 4. (a) Trajectory of PAANa hydrogels polymerized using 0, 30, and 50% hexane in 2.5 V/cm electric fields. At (b) 90 and (c) 180 s, a significant pH gradient has been generated across the hydrogel to initiate bending. These results suggest the formation of a pH gradient has a larger effect on the bending trajectory of porous hydrogels. Error bars represent the standard error of the mean (s.e.m.) of the measurements, * indicates $p < 0.01$. Scale bar = 2 mm.
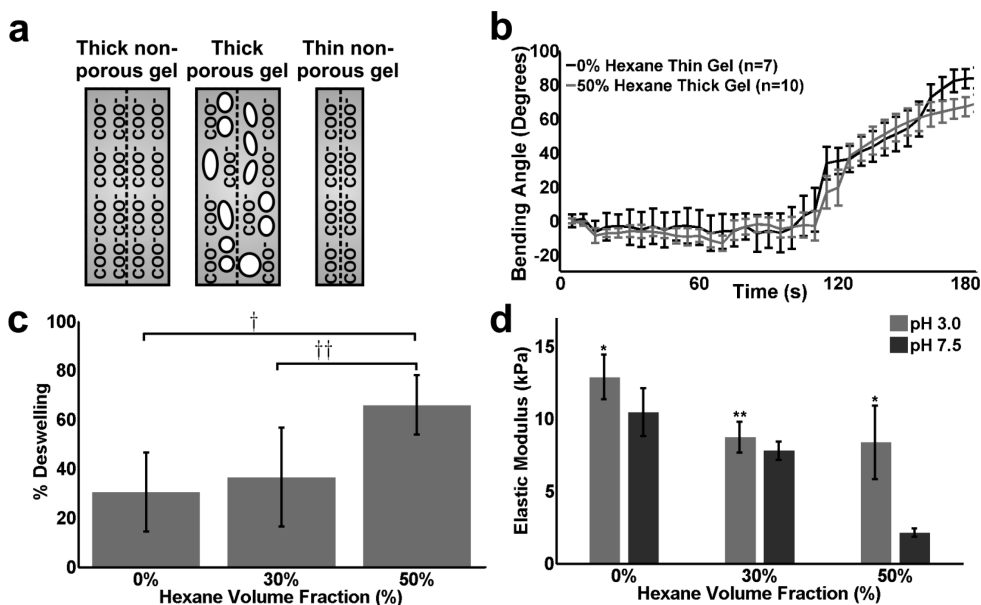

FIGURE 5. (a) Hypothetical cross-sectional area and volume density of the PAANa gel across the gel slab. When nonporous gels were engineered to be 50% thinner, these gels followed the same trajectory as the ~2 mm thick porous hydrogels produced using a 50% emulsion. Error bars represent the standard error of the mean (s.e.m.) of the measurements. The decreased volume density of porous hydrogels allows the gels to (c) deswell and (d) stiffen to a much larger extent than nonporous hydrogels. A student's 2-sample t test was utilized to test for statistical significance, where † corresponds to $p > 0.001$, †† indicates $p > 0.005$, * indicates $p > 0.01$, and ** indicates $p > 0.05$.

emulsion (Figure 3e−i) produced average bending angles of $62.8 \pm 16.2°$ ($n = 7$, s.d.) and PAANa gels polymerized in a 50% hexane emulsion (Figure 3e,j−m) generated bending angles of $70.4 \pm 20.0°$ ($n = 16$, s.d.). The maximum bending angle of the PAANa gels polymerized in 30% and 50% hexane were found to be statistically significant from the nonporous PAANa ($p < 0.01$). In general, the standard deviation was approximately 30% of the average maximum bending angle achieved, indicating the maximum bending

angle typically varied by 30%. As shown in Figure 4a, the variations in bending angle trajectory were generally 20−30% of the mean bending angle at each time point, further indicating that a 20−30% error exists in reproducibility. The PAANa gels polymerized with 30 and 50% hexane may be statistically insignificant because coalescence of droplets often occurs in an emulsion at high-volume fractions (>30%), such that coalescence of hexane droplets during polymerization may occur (19). Overall, these results indicate that

the bending angle of PAANa gels can be improved by >60% when an emulsion templating technique is utilized.

Interestingly, despite the increased actuation of porous PAANa hydrogels, during the first 60–100 s after an electric field was applied, the trajectory of the PAANa gels was strikingly similar to the nonporous hydrogels (Figure 4a). When 2.5 V/cm was applied for 3 min, the porous hydrogels only bent to a greater extent than the nonporous hydrogels after an electric field was applied for 120–130 s, when a strong pH gradient had been established across the hydrogel (Figure 4b,c). Images of pH gradients indicated that a larger pH gradient was created across the hydrogel over time (Figure 4b,c). The pH gradient yielded a spatial gradient of COOH and COO$^-$ groups within the hydrogel. As more COOH groups were created within the hydrogel on the anode (low pH) side of the gel relative to the cathode (high pH) side, the polymer compressed on the COOH dominant (anode) side (13, 16), initiating a large bending angle. Overall, these results demonstrate that an acidic pH gradient (high H$^+$ concentration) enhances the bending trajectory of porous hydrogels to a much larger extent than nonporous hydrogels.

Effects of Hydrogel Thickness on Hydrogel Bending. Because polyacrylate polymer bending is initiated by protonation of the anode side of the gel (13, 14, 16, 17), we hypothesized that a smaller concentration of COO$^-$ groups must be protonated across a porous gel slab as compared to a nonporous gel slab to generate bending (Figure 5a). The decreased number of COO$^-$ groups across a porous gel slab that must be converted to COOH groups to generate bending is analogous to the lower number of COO$^-$ groups that must be protonated in a thinner gel slab to initiate bending (Figure 5a). In fact, we observe that 50% thinner, nonporous hydrogels follow the same bending trajectory as porous hydrogels produced in a 50% hexane emulsion (Figure 5b). Therefore, the bending is critically dependent on the cross-sectional area, because the cross-sectional area determines the concentration of COO$^-$ groups across the gel that must be protonated to form COOH groups and initiate bending.

Effects of Deswelling on Hydrogel Bending. The density and cross-sectional area of the PAANa gels also influence their deswelling properties, because porous hydrogels have a large percentage of void space compared to solid hydrogels. After equilibration in a heavily buffered pH 7.5 solution and placement in a pH 3.0 solution, porous hydrogels created in a 50% emulsion deswelled two times more than nonporous hydrogels (Figure 5c). In particular, porous hydrogels generated in a 50% emulsion deswelled 66 ± 12% (n = 8, s.d.), whereas porous hydrogels generated in a 30% emulsion deswelled 36 ± 30% (n = 8, s.d.) and nonporous hydrogels deswelled 30 ± 16% (n = 8, s.d.). In effect, these results indicate that porous hydrogels have enhanced actuation properties because they are able to deswell and contract to a larger extent in the presence of low pH solutions.

Additionally porous hydrogels were less stiff and underwent concomitantly larger increases in stiffness when exposed to low pH solutions (Figure 5d). For instance, when placed in a pH 7.5 solution, the nonporous hydrogels had an elastic modulus of 10.5 ± 1.7 kPa, as compared to the PAANa gels polymerized in a 30% and 50% emulsion which had elastic moduli of 7.8 ± 0.6 kPa and 2.15 ± 0.2 kPa, respectively. Yet, when placed a pH 3.0 solution, nonporous hydrogels increased in stiffness by 18%, whereas PAANa gels polymerized in a 50% emulsion increased in stiffness by 295%. This result indicates that the enhanced deswelling of porous hydrogels allows them to stiffen to a larger extent than nonporous hydrogels, thereby improving their bending when exposed to an acidic pH gradient.

In summary, we have shown that large bending angles of PAANa gels can be achieved using an emulsion templating method. Porous hydrogels are favorable for actuation because the cross-sectional area of the gels is such that a smaller pH gradient is required across the hydrogel to protonate COO$^-$ groups and initiate bending. Moreover, porous hydrogels bend to a larger extent because of their increased flexibility, decreased COO$^-$ concentration across the gel slab, and enhanced deswelling mechanisms. The use of porous hydrogels can be implemented in novel soft robotic actuators to enhance actuation of artificial muscle constructs.

Supporting Information Available: Additional information on the stress–strain ratio of the hydrogels (PDF). This material is available free of charge via the Internet at http://pubs.acs.org.

REFERENCES AND NOTES

(1) Baughman, R. H. *Science* **2005**, *308*, 63–65.
(2) Madden, J. D. W.; Vandesteeg, N. A.; Anquetil, P. A.; Madden, P. G. A.; Takshi, A.; Pytel, R. Z.; Lafontaine, S. R.; Wieringa, P. A.; Hunter, I. W. *IEEE J. Oceanic Eng.* **2004**, *29*, 706–728.
(3) Onoda, M.; Kato, Y.; Shonaka, H.; Tada, K. *Electron. Eng. Jpn.* **2004**, *149*, 7–13.
(4) Moschou, E. A.; Peteu, S. F.; Bachas, L. G.; Madou, M. J.; Daunert, S. *Chem. Mater.* **2004**, *16*, 2499–2502.
(5) Moschou, E. A.; Madou, M. J.; Bachas, L. G.; Daunert, S. *Sens. Actuators, B* **2006**, *115*, 379–383.
(6) Otero, T. F.; Broschart, M. *J. Appl. Electrochem.* **2006**, *36*, 205–214.
(7) Takashima, W.; Kanamori, K.; Pandey, S. S.; Kaneto, K. *Sens. Actuators, B* **2005**, *110*, 120–124.
(8) Bay, L.; West, K.; Sommer-Larsen, P.; Skaarup, S.; Benslimane, M. *Adv. Mater.* **2003**, *15*, 310–313.
(9) Jager, E. W. H.; Smela, E.; Inganas, O. *Science* **2000**, *290*, 1540–1545.
(10) Osada, Y.; Okuzaki, H.; Hori, H. *Nature* **1992**, *355*, 242–244.
(11) Shiga, T.; Hirose, Y.; Okada, A.; Kurauchi, T. *Abstr. Pap. Am. Chem. S.* **1989**, *197*, 154–158.
(12) Hirai, T.; Nemoto, H.; Hirai, M.; Hayashi, S. *J. Appl. Polym. Sci.* **1994**, *53*, 79–84.
(13) Doi, M.; Matsumoto, M.; Hirose, Y. *Macromolecules* **1992**, *25*, 5504–5511.
(14) Yao, L.; Krause, S. *Macromolecules* **2003**, *36*, 2055–2065.
(15) LeDuc, P. R.; Robinson, D. R. *Adv. Mater.* **2007**, *19*, 3761–3770.
(16) Shiga, T. *Adv. Polym. Sci.* **1997**, *134*, 131–163.
(17) Grimshaw, P. E.; Nussbaum, J. H.; Grodzinsky, A. J.; Yarmush, M. L. *J. Chem. Phys.* **1990**, *93*, 4462–4472.
(18) Tokuyama, H.; Kanehara, A. *Langmuir* **2007**, *23*, 11246–11251.
(19) Mason, T. G.; Bibette, J.; Weitz, D. A. *Phys. Rev. Lett.* **1995**, *75*, 2051–2054.

AM900755W